A Chloride Channel at the Basolateral Membrane of the Distal-convoluted Tubule: a Candidate ClC-K Channel

Stéphane Lourdel, Marc Paulais, Pedro Marvao, Antoine Nissant, and Jacques Teulon

Laboratoire de Physiologie, CNRS-FRE 2468, Institut des Cordeliers, 75270 Paris, France

ABSTRACT The distal-convoluted tubule (DCT) of the kidney absorbs NaCl mainly via an Na^+-Cl^- cotransporter located at the apical membrane, and Na^+, K^+ ATPase at the basolateral side. Cl^- transport across the basolateral membrane is thought to be conductive, but the corresponding channels have not yet been characterized. In the present study, we investigated Cl^- channels on microdissected mouse DCTs using the patch-clamp technique. A channel of ~9 pS was found in 50% of cell-attached patches showing anionic selectivity. The NP_o in cell-attached patches was not modified when tubules were preincubated in the presence of 10^{-5} M forskolin, but the channel was inhibited by phorbol ester (10^{-6} M). In addition, NP_o was significantly elevated when the calcium in the pipette was increased from 0 to 5 mM (NP_o increased threefold), or pH increased from 6.4 to 8.0 (NP_o increased 15-fold). Selectivity experiments conducted on inside-out patches showed that the Na^+ to Cl^- relative permeability was 0.09, and the anion selectivity sequence $Cl^- \sim I^- > Br^- \sim NO_3^- > F^-$. Intracellular NPPB ($10^{-4}$ M) and DPC (10^{-3} M) blocked the channel by 65% and 80%, respectively. The channel was inhibited at acid intracellular pH, but intracellular ATP and PKA had no effect. ClC-K Cl^- channels are characterized by their sensitivity to the external calcium and to pH. Since immunohistochemical data indicates that ClC-K2, and perhaps ClC-K1, are present on the DCT basolateral membrane, we suggest that the channel detected in this study may belong to this subfamily of the ClC channel family.

KEY WORDS: chloride channel • ClC-K • kidney • PKC • patch-clamp

INTRODUCTION

The distal-convoluted tubule (DCT),* a heterogeneous segment in most species, contributes to urine dilution, to the reabsorption of NaCl and calcium, and to the secretion of potassium (Reilly and Ellison, 2000). Na^+ absorption in the DCT mainly takes place via a thiazide-sensitive Na^+-Cl^- cotransport, and amiloride-sensitive Na^+ channels. Apical Na^+/H^+ and Cl^-/organic anion exchanges operating in parallel have also been proposed (Wang et al., 1993). Na^+ leaves the cell from the basolateral side via Na^+, K^+ ATPase, whereas Cl^- is thought to pass through a Cl^--selective conductance, and possibly the K^+-Cl^- cotransport. This K^+-Cl^- cotransport system was initially proposed by Greger and Velazquez (1987) on the basis that no Cl^- conductance was detected in the basolateral membrane of the rabbit DCT. However, using the same technique of the isolated, microperfused tubule on the rabbit DCT, Yoshitomi et al. (1989) did detect Cl^- conductance, which was best revealed under conditions of reduced K^+ conductance. To date, no published data is available about basolateral Cl^- channels in the native DCT, although there have been reports concerning Cl^- currents in DCT-cultured cells (Rubera et al., 1997, 1999), or Cl^- channels in the apical membrane of DCT-cultured cells (Poncet et al., 1994) and in membrane vesicles (Sauvé et al., 2000).

Independent evidence of the presence of Cl^- channels within this part of the renal tubule has emerged from molecular biology and immunohistochemistry, so that it is generally accepted that there are ClC-K Cl^- channels embedded within the DCT basolateral membrane (Uchida, 2000; Jentsch et al., 2002). In addition, it has been shown that ClC-Kb (the human ortholog of rodent ClC-K2) is implicated in a variant of the Bartter syndrome, and may induce a Bartter-Gitelman mixed phenotype in some cases (Simon et al., 1997; Konrad et al., 2000). Thus, the Cl^- channels detected in the DCT basolateral membrane could correspond to ClC-K channels. The electrophysiological properties of the ClC-K channels have not been investigated in detail using heterologous expression systems, and unfortunately no information is available at the single-channel level (see Uchida, 2000; Jentsch et al., 2002). However, the earlier studies from Uchida and Jentsch's laboratories, plus the more recent experiments with the Barttin

Pedro Marvao's present address is Department de Fisiologia, Faculdade de Ciencias Medicas de Lisboa, Universidade Nova de Lisboa, Campo Martires da Patria, 130, 1169-056 Lisboa, Portugal.

Address correspondence to Jacques Teulon, Laboratoire de Physiologie et Génomique des Cellules Rénales, CNRS-FRE 2468, Institut des Cordeliers, 15 rue de l'Ecole de Médecine, 75270 Paris CEDEX 06, France. Fax: (33) 146 33 41 72; E-mail: jacques.teulon@bhdc.jussieu.fr

*Abbreviations used in this paper: DCT, distal-convoluted tubule; NCC, Na^+-Cl^- cotransporter; PS, physiological saline.

J. Gen. Physiol. © The Rockefeller University Press • 0022-1295/2003/04/287/14 $8.00
Volume 121 April 2003 287–300
http://www.jgp.org/cgi/doi/10.1085/jgp.200208737

regulatory subunit, firmly establish two reliable sets of properties. These are the permeability sequences, and the sensitivities to external pH and calcium (Adachi et al., 1994; Uchida et al., 1993, 1995; Waldegger and Jentsch, 2000; Waldegger et al., 2002; Estevez et al., 2001). These properties can be used to compare endogenous Cl^- channels in the native DCT with ClC-Ks. Accordingly, our study was designed to record and characterize Cl^- channels on the basolateral membrane of microdissected DCT tubules using the patch-clamp technique. We found only one type of Cl^- channel, and this is definitely distinct from two Cl^- channels identified in the cortical thick ascending limb (Paulais and Teulon, 1990; Guinamard et al., 1995, 1996; Marvao et al., 1998; Reeves et al., 2001). The Cl^- channel on the DCT basolateral membrane has properties compatible with ClC-K2.

MATERIALS AND METHODS

Isolation of Renal Tubules

The experiments were performed under licence no. 7427 of the Veterinary Department of the French Ministry of Agriculture. Male mice (15–20 g; Harlan) were killed by cervical dislocation. The DCTs were isolated from the kidneys after collagenase treatment (Worthington CLS II, 300 U/ml) as described previously (Lourdel et al., 2002). The mouse DCT is a heterogeneous structure (Reilly and Ellison, 2000), but several studies have shown that the first section of the DCT (DCT1) consists mainly of distal cells, that have the Na^+-Cl^- cotransporter (NCC), but not the epithelial Na^+ channel (see also Reilly and Ellison, 2000; Loffing et al., 2001). Consequently, in order to patch mainly DCT1 cells, the patch-clamp recordings were done approximately within 300 μm from the beginning of the DCT, after the postmacula densa short TAL-like segment.

Solutions and Chemicals

The tubules were initially bathed with physiological saline (PS) containing (in mM) 140 NaCl, 4.8 KCl, 1 $CaCl_2$, 1.2 $MgCl_2$, 10 glucose, 10 HEPES, and adjusted to pH 7.4 with NaOH. Unless otherwise stated, the patch pipettes were filled with a solution containing (in mM): 145 NaCl, 1 $CaCl_2$, 1.2 $MgCl_2$, 10 glucose, 10 HEPES, and adjusted to pH 7.4 with NaOH. For cell-attached patch recordings, we also used pipette solutions in which 145 mM CsCl, or 145 mM NMDG-Cl, or 100 mM Na-gluconate was substituted for NaCl. Patches were excised from the DCTs directly into PS or, alternatively, into a solution containing no calcium and supplemented with 2 mM EGTA. The solutions used to characterize channel properties in the inside-out configuration contained 2 mM EGTA and no calcium (except where otherwise stated). Anion versus cation selectivity was tested using a low NaCl solution in which the NaCl concentration was reduced to 14 mM (with 260 mM sucrose) and no KCl added. DPC, at a concentration of 0.5 M, (Fluka), NPPB, at a concentration of 0.1 M (Sigma-Aldrich), PMA (Sigma-Aldrich) and 4αPDD (Calbiochem), at a concentration of 0.02 M, were dissolved in DMSO. DMSO (at the maximal concentration of 0.2% used for 10^{-3} M DPC) had no effect on channel activity ($n = 3$). The catalytic subunits of the cyclic AMP dependent protein kinase A were from Sigma-Aldrich and Promega.

Current Recordings

Single-channel currents were recorded from patches of basolateral membranes using the cell-attached and excised, inside-out configurations of the patch-clamp technique (Hamill et al., 1981). Patch-clamp pipettes were pulled in two stages with a Kopf puller using borosilicate glass (GC150T; Harvard Apparatus). They were coated with Sylgard and polished just before use. The PS-filled pipettes had a mean resistance of 4.9 ± 0.2 MΩ ($n = 65$). Currents were recorded with List LM-EPC7 or Bio-logic RK 400 patch-clamp amplifiers, monitored using Axoscope software (Axon Instruments, Inc.) and stored on digital audio tape (Sony DTR-1205; Bio-logic). In the cell-attached configuration, the clamp potential applied with respect to the bath (V_c) is superimposed on the spontaneous membrane potential. Potentials across cell-attached and excised membrane patches were corrected for liquid junction potentials as described by Barry and Lynch (1991). The liquid junction potentials were measured directly using a procedure described previously (Paulais and Teulon, 1990). The junction potentials (compared with PS and expressed in absolute values) were 8.5 mV for the NaCl-diluted solution, 6 mV for the 145 mM NMDG-Cl solution, 5 mV for the 100 mM Na-gluconate solution, and <5 mV for the other experimental solutions. Currents carried by anions moving from the outer to the inner face of the patch membrane were considered positive, and are shown as upward deflections in the current tracings. The experiments were performed at room temperature (22–27°C).

Analysis of Channel Activity

Single-channel current recordings were filtered at 300 or 500 Hz low-pass by an 8-pole Bessel filter (LPBF-48DG; NPI Electronic) and digitized at a sampling rate of 1–2 kHz using a Digidata 1200 analogue-to-digital converter and Axoscope software (Axon Instruments, Inc.). Channel activity was measured from digitized stretches of recording lasting at least 30 s using custom-built software (T. Van Den Abbeele). For this purpose, the time-averaged current passing through the channels on the patch, $<I>$, was calculated from current amplitude histograms, taking the closed current level as reference. NP_o and P_o were estimated from the equation $<I> = NP_o\, i$, where N, P_o, and i are the number of channels in the patch, the open state probability and the amplitude of the unit current, respectively. The maximum number of channels simultaneously open was determined by a visual inspection of the whole recording in order to calculate P_o. In cell-attached patches, we estimated the closed current level by inhibiting Cl^- channel activity. The experimental procedure took advantage of the fact that this channel is inhibited at intracellular acid pH. The tubule under study was superfused by a solution containing 20 mM Na-acetate, which induced a maximum intracellular acidification of 0.35 ± 0.03 U pH ($n = 4$) within 15 s. The time necessary for half-recovery of the intracellular pH was 68 ± 12 s. The channels were usually inhibited very efficiently and rapidly; however, there was no reversal of the inhibition.

Very few recordings had only one active channel, and the kinetics of the channel appeared to be very slow. Thus, we analyzed the opening and closure of the channel by merging all useable recordings available. The data were filtered at 300 Hz and digitized at a sampling rate of 1 kHz. The TAC single-channel analysis software from Bruxton Corporation was used.

Ion Selectivity

The Na^+ permeability ratio P_{Na}/P_{Cl} was estimated using low NaCl bath solution containing 14 mM NaCl. For anion selectivity, 130 mM NaCl on the bath side was replaced by an equivalent amount of a sodium salt of the test anion (designated as X^- in the follow-

ing equations). The activity coefficients used in the calculations were 0.89 for the low NaCl solution and 0.76 for all other solutions (Robinson and Stokes, 1965). When it was not possible to measure the unit currents beyond the reversal potentials (E_r), we calculated the permeability ratios from E_r. Individual E_r values were determined from the linear regression of the experimental data points. The voltage equation of Goldman, Hodgkin, and Katz used for these calculations was as follows (when testing the cation/anion permeability, $[X^-]$ was nullified):

$$E_r = \frac{RT}{F}\ln\frac{P_{Cl}[Cl^-]_i + P_x[X^-]_i + P_{Na}[Na^+]_p}{P_{Cl}[Cl^-]_p + P_{Na}[Na^+]_i}, \quad (1)$$

where the p and i subscripts refer to the pipette and the intracellular sides of the patch, respectively.

When it was possible to detect openings at more negative potentials than E_r, the P_{Na}/P_{Cl} and P_X/P_{Cl} ratios were derived by fitting the experimental data points to the current equation of Goldman, Hodgkin, and Katz. The following equation was used (when testing the cation/anion permeability, $[X^-]$ was nullified):

$$i = gV_c\left[1 + \frac{P_{Na}}{P_{Cl}}\frac{[Na^+]_i - [Na^+]_p e^{-\frac{FV_c}{RT}}}{[Cl^-]_p} - \left(\frac{P_X}{P_{Cl}}\frac{[X^-]_i}{[Cl^-]_p} + \frac{[Cl^-]_i}{[Cl^-]_p}\right)e^{-\frac{FV_c}{RT}}\right] \Big/ \left(1 - e^{-\frac{FV_c}{RT}}\right), \quad (2)$$

where

$$g = \frac{P_{Cl}F^2}{RT}[Cl^-]_p \cdot g,$$

is the unit conductance in symmetrical conditions for Cl^-.

Measurement of Intracellular pH and Calcium

The pH_i and the $[Ca^{2+}]_i$ were measured using video-enhanced fluorescence microscopy and image processing (Argus-50; Hamamatsu Photonics K.K.). Images of BCECF-loaded DCT segments were obtained, ratioed, and converted to pH_i values as described previously (Marvao et al., 1998). A similar approach was used for $[Ca^{2+}]_i$ measurements with Fura-2, except that DCTs were epi-lluminated at 340 and 380 nm, and the emitted light was detected at 510 nm. Ratioed images were then converted to $[Ca^{2+}]_i$ values using an in vitro calibration curve. All images were corrected for shading, and background fluorescence was not detectable.

RT-PCR

RNAs were extracted from pools of 20–40 DCTs (0.3–0.5 mm) as described previously (Chomczynski and Sacchi, 1987). Expression of mRNA encoding the chlorothiazide-sensitive Na^+-Cl^- transporter NCC (U 61085) and the ClC-K1 (TC178640) and ClC-K2 (AF124847) Cl^- channels was assessed by RT-PCR, using the following primers: NCC sense (5′-TCTCACCCTCCTCATCCCCTATCT-3′) and antisense (5′-CAGAGCAGCATCCCGAGAGTAATC-3′), bases 2475 and 2845, respectively; CLC-K1 sense (5′-GACCCTTCAGGCGCTGTTCGT-3′) and antisense (5′-CGTAAACCGGGGTGAGATTTGTCC-3′), bases 2101 and 2407, respectively; CLC-K2 sense (5′-CTGGTGGGCGTTGTAAAAAGGAC-3′) and antisense (5′-GGGAGGATTGGTCAGGGTTGAA-3′), bases 1809 and 2072, respectively. RT was performed for 2 h at 37°C in a final volume of 10 μl in the presence of RNAs from 0.25 mm tubule length, random primers (pd(N)6 5 μM, Roche Diagnostics), $MgCl_2$ (2 mM), dNTPs (500 μM), and 100 U Superscript™ II reverse transcriptase (Invitrogen). PCR was performed in the same tube in a final volume of 100 μl after adding the sense and antisense primers (10 pmoles), and 2.5 U Taq DNA polymerase (QIAGEN). Samples were subjected to 35 cycles of three temperature steps: 94°C, 30 s; 59°C, 30 s; 72°C for 1 min, except for the last cycle in which the elongation lasted 10 min. For both ClC-K1 and ClC-K2, the nature of the PCR product (expected to be 330 and 285 bp, respectively) was confirmed using the specific restriction enzymes Bst N1 and Eco RV (Biolab, Inc.).

Statistics

Results are given as means ± SEM for the indicated number of measurements (n). Origin software (Microcal) was used to fit the data points to equations. The statistical significance was evaluated by Student's t test or Mann-Whitney Rank Sum test when necessary, using Sigmastat software (SPSS). $P < 0.05$ was considered significant.

RESULTS

Conductive Properties of the Channel in Cell-attached Patches

We recorded two types of channel from cell-attached patches formed on the basolateral membranes of DCTs when we used PS in the pipette and bath. One was a nonselective cation channel previously reported from our laboratory (g = 27.8 ± 1.3 pS; E_r = 44.8 ± 4.9 mV, n = 20) (Chraibi et al., 1994; Lourdel et al., 2002). The second channel was the subject of this study. Typical activity is shown in Fig. 1 A. Two characteristic properties are worth emphasizing: (a) most of the openings were long, that is in the second or subsecond range. This is apparent on the tracings in Fig. 1 A. A particularly long opening in a cell-attached patch is shown in Fig. 1 C. Unfortunately, this channel usually occurred in clusters, which made it impossible to carry out a quantitative analysis of the kinetics in the cell-attached configuration. (b) One substate with an amplitude half as great as full opening occurred quite frequently. Two such substates (arrows) are indicated on the channel current traces in Fig. 1 A. We were able to analyze the substates in some detail in both cell-attached, and excised patches (see relevant section of RESULTS). The mean current-voltage relationship was linear (Fig. 1 B) and showed a unit conductance of 9.5 ± 0.3 pS (n = 25) in the cell-attached mode. The reversal potential (2.1 ± 2.0 mV, n = 25) was close to zero. We qualitatively estimated the ionic selectivity in separate cell-attached patches by testing the effects on the reversal potential of changing the composition of the pipette solution. When CsCl or NMDG-Cl (140 mM) was substituted for NaCl, there was no significant change in the reversal potential (CsCl: E_r = 2.41 ± 1.8 mV, n = 5; NMDG: −1.0 ± 1.9 mV, n = 5). In contrast, when 100 mM NaCl was replaced by Na gluconate, the reversal potential was shifted to the right by 31.7 ± 3.7 mV (n = 4), indi-

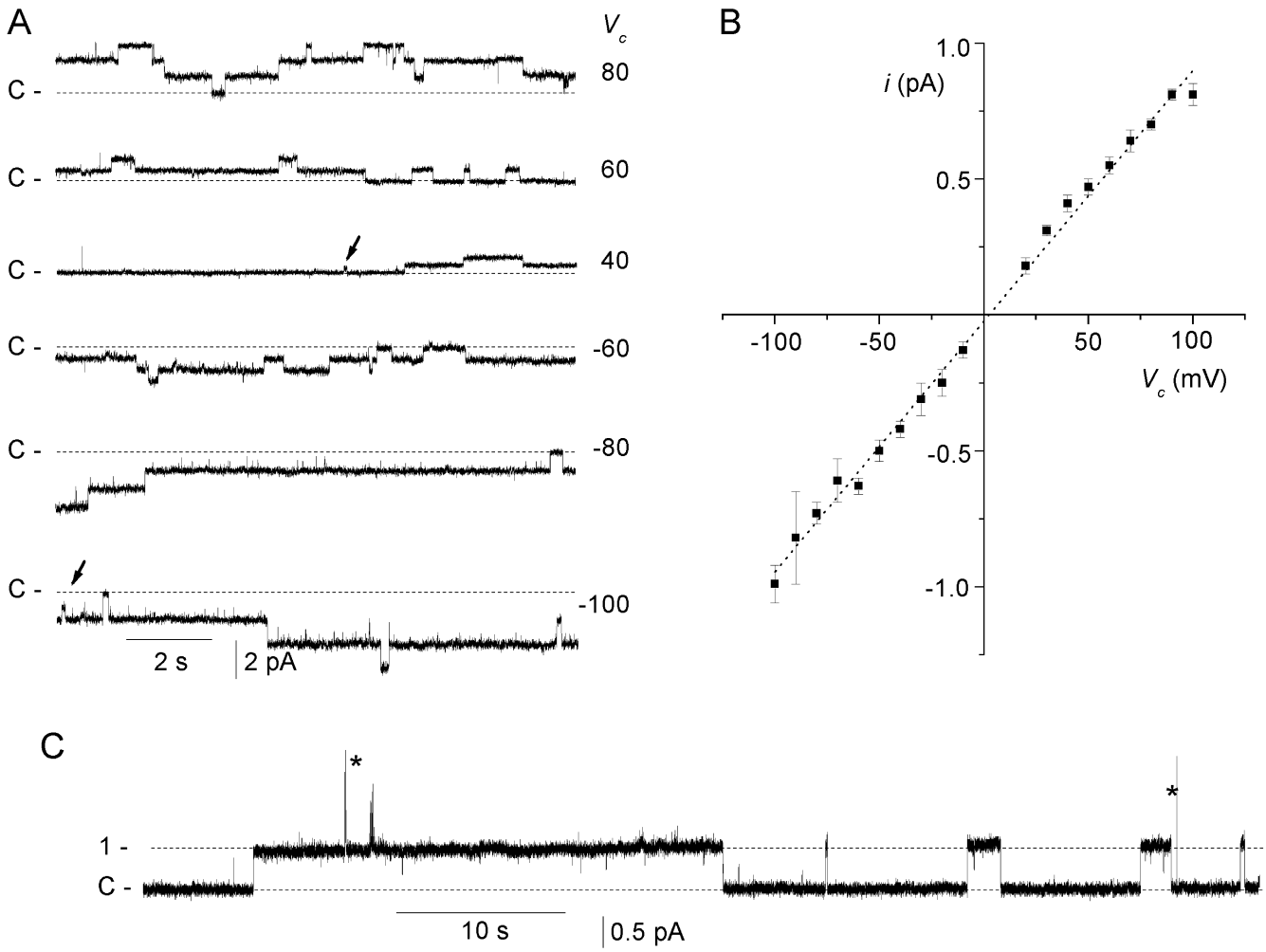

FIGURE 1. Conductive properties in the cell-attached configuration. (A) Representative current recordings from a membrane patch formed on a DCT bathed with physiological saline solution (PS), at various clamped potentials (V_c, as indicated on the right side of each trace). The pipette solution was PS. The arrows point to sublevel (half-amplitude) openings. The dotted line labeled with C in this and subsequent figures denotes the closed current level. (B) Mean single-channel current (*i*)/voltage (*Vc*) relationship obtained under the same condition. Each point is the average of 3–17 determinations from 25 separate patches. SEM is shown as error bars when larger than symbols. C) Excerpt from a channel current recording in the cell-attached mode showing a particularly lengthy opening (~28 s). The asterisks indicate noise artifacts.

cating Cl^- selectivity. No change in the unit conductance was detected in any of the three conditions. The fact that $E_r \sim 0$ mV with PS in the pipette indicates that Cl^- is close to equilibrium, possibly because the Na^+-Cl^- cotransport is largely inactive under our experimental conditions.

Channel Activity in Cell-attached Patches

Visual inspection of the recordings did not reveal any clear evidence of voltage dependence. However, we observed that channel activity spontaneously decreased in some cases when the *Vc* was set to a high positive potential (>80 mV). Under the conditions specified in the previous section, the channel was encountered in 54% of patches (53 out of 98 patches) and this frequency was not increased when we preincubated the DCTs in a solution containing 10^{-5} M forskolin for 15 min or more (see Fig. 2 A; 54%, 24 out of 44 patches). We designed experiments to assess the number of channels per patch under the two conditions. We know from previous studies of small Cl^- channels in the cortical thick ascending limb that the closed current level cannot be accurately determined in cell-attached patches without inhibiting channel activity (Guinamard et al., 1996; Marvao et al., 1998). This is due to their high P_o and slow kinetics. Since the DCT Cl^- channel is inhibited at intracellular acid pH (see below, relevant section of RESULTS), we inhibited the channels in the cell-attached mode by superfusing Na-acetate (20 mM, see MATERIALS AND METHODS) around the tubule being patched;

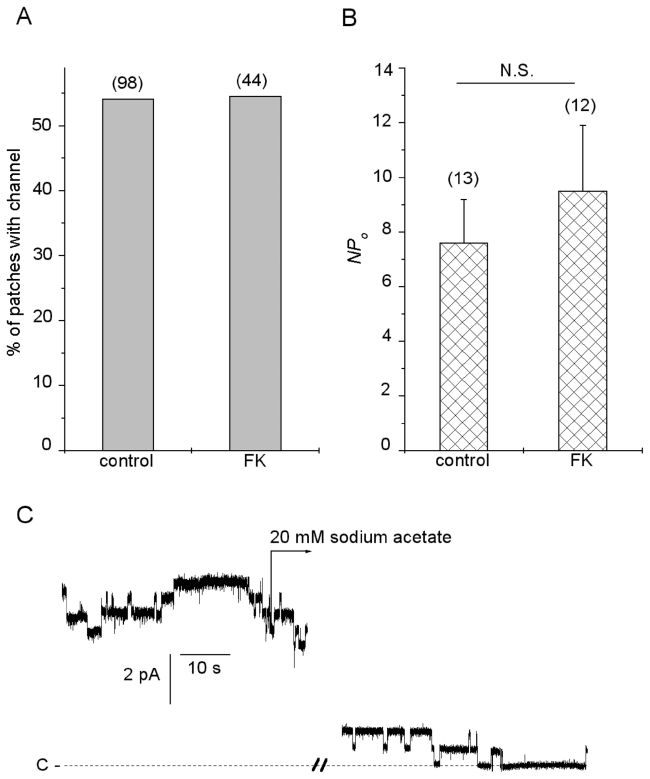

FIGURE 2. Assessment of channel activity in cell-attached patches: lack of effect of preincubating tubules with 10^{-5} M forskolin (FK). (A) Percentage of patches containing 9-pS channels under control and stimulated (FK) conditions. The tubules were bathed with 10^{-5} M forskolin for at least 10 min. (B) Channel activity (NP_o) under the same two conditions. The measurement was done at the beginning of the recording over 30–90 s depending on the patch. The number of observations is indicated between brackets. (C) The effect on channel activity of superfusing 20 mM sodium acetate around the tubule being patched. This cell-attached patch contained 11 channels. The nonreversible inhibition induced by intracellular acidification allows estimating the closed current level. This in turn is used to calculate the time-averaged current and NP_o.

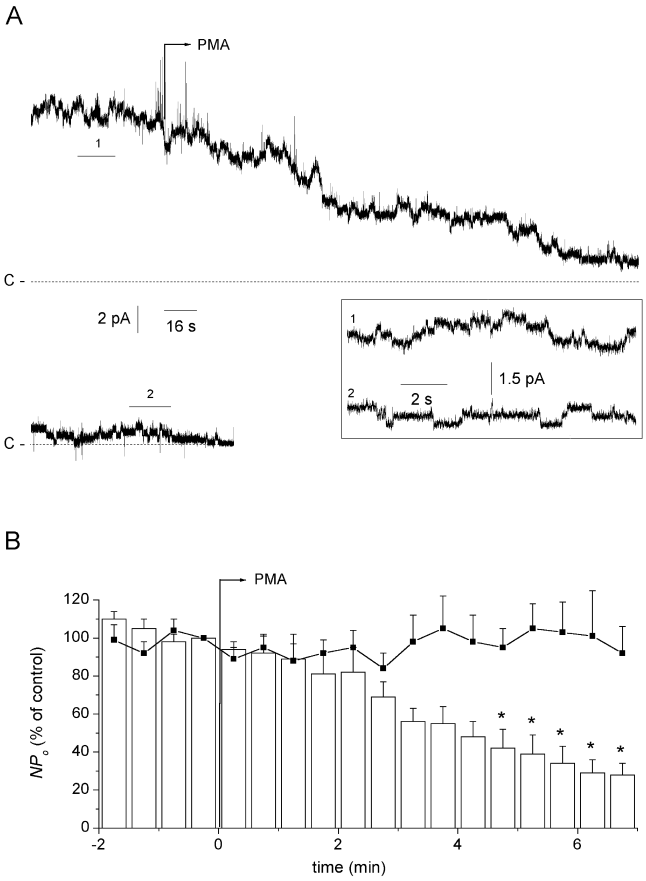

FIGURE 3. Inhibition of the DCT Cl^- channel induced by the phorbol ester PMA. (A) The figure shows channel current recording from a cell-attached patch at a clamp potential of 60 mV (PS in the pipette and in the bath). The application of 1 μM PMA induced a gradual decrease in channel activity, which eventually resulted in almost total inhibition for this particular recording, which had 21 active channels. (B) The histograms show the average time course of channel activity (NP_o) in the presence of PMA (1 μM, bars), which stimulates PKC, or of 4αPDD (1 μM, filled squares), an inactive analogue of PMA. The NP_o are expressed as a percentage of the NP_o measured over the 30 s preceding stimulation. The time at which the drug was applied is labeled as zero. Each point is the mean of 8 (PMA) or 10 (4αPDD) observations, except at times 6.5 and 7.0 min (PMA, $n = 6$; 4αPDD, $n = 7$). The NP_os measured between 5 and 7 min in the two situations were analyzed using ANOVA and Student-Newman-Keuls method, and were significantly different (asterisks).

the time necessary to reduce the channel activity by 50% was 66 ± 6 s ($n = 31$). The inhibition was usually irreversible. A typical experiment is shown in Fig. 2 C. On-cell channel activity was first recorded under control conditions (no Na-acetate) for about 1 min in order to determine the mean channel current, and 20 mM Na-acetate was subsequently superfused around the tubular fragment. Channels closed progressively until a stable current level was reached, which was taken to be an estimate of the closed level. The number of channels per patch varied considerably from patch to patch, ranging from 1 to 15 channels per patch, but as seen in Fig. 2 B, this number does not appear to differ in cAMP-stimulated and control tubules (control, $NP_o = 7.6 \pm 1.6$, $n = 13$; FK-stimulated, $NP_o = 9.5 \pm 2.4$, $n = 12$, NS).

Inhibition of the Channel Caused by PKC Stimulation

We investigated whether the PKCs might be involved in the regulation of the DCT Cl^- channel by monitoring the NP_o in the cell-attached configuration while superfusing PMA (1 μM), an activator of PKC, around the DCT being patched. The effect of PMA is illustrated in Fig. 3 A. Despite the fact that a slight decrease in channel activity occurred during the control period, marked inhibition in the presence of PMA was clearly apparent after a 1-min delay, and PMA decreased the NP_o to 13% of control after 4 min (period labeled 2 in Fig. 3 A). However,

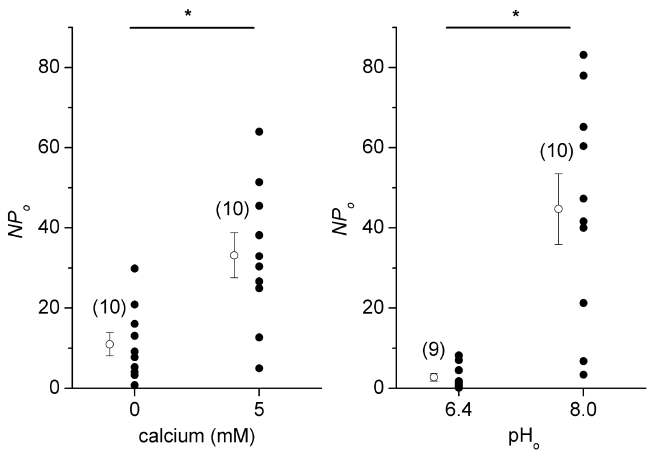

FIGURE 4. Effects on channel activity of changing the calcium concentration or the pH (pH_o) in the pipette. The histograms show individual NP_o measurements (solid circles) and means ± SEM (open circles) under the various conditions for the pipette solution (no calcium or 5 mM calcium at pH 7.4; pH 6.4 or pH 8.0 in the presence of 1 mM calcium). The NP_o were measured as indicated in Fig.2. The differences were statistically significant at 0.002 (calcium) and 0.001 (pH_o) levels. The number of observations is given between brackets.

the delay and the degree of inhibition were variable from patch to patch. The mean time course of channel activity (NP_o) in the presence of PMA is shown in Fig. 3 B (eight patches). Regression for NP_o over time, calculated between 2.5 and 7.0 min, gave a slope of −11 ± 2% of control NP_o/30 s ($P < 0.001$). As a control, we challenged tubules with 4αPDD, an analogue of PMA that does not activate PKC (10 patches). As shown in Fig. 3 B, a small decrease in channel activity was observed during the control period, but 4αPDD had no inhibitory effect, and the NP_o remained high all along. For instance, the NP_o after exposure to 4αPDD for 7 min (92 ± 7% of control, n = 7, see Fig. 3 B) was significantly different from that after exposure to PMA for the same length of time (29 ± 6% of control, n = 6, Fig. 3 B). Furthermore, regression analysis between 2.5 and 7.0 min showed that the NP_o was independent of time ($P = 0.83$). The inhibition caused by PMA was not indirectly linked to changes in $[Ca^{2+}]_i$, since there was no difference before and after superfusing the tubules with PMA for 10 min (control, 31 ± 6 nM; PMA, 39 ± 9 nM, n = 3; NS).

We also investigated the possible effects of intracellular Ca^{2+} directly, by superfusing tubules with the calcium ionophore ionomycin (10 μM) in the presence of 1 mM calcium for 7 min (n = 5). The Ca^{2+} response to ionomycin was evaluated in separate experiments: $[Ca^{2+}]_i$ increased from 100 ± 9 nM to 180 ± 12 nM (n = 4) over the same period of time. The time course of the NP_o in the presence of ionomycin was indistinguishable from that observed when PS (containing no ionomycin) was superfused around the tubule (n = 5). For instance, the NP_os (in percentage of the NP_o before test) after exposure to ionomycin for 6 (84 ± 8%, n = 5) or 7 min (73 ± 12%, n = 4) were not significantly different from the NP_os after superfusion with PS for 6 (96 ± 35%, n = 5) or 7 min (82 ± 35%, n = 5).

Dependence on External pH and Calcium

It has been shown that ClC-K channels expressed in *Xenopus* oocytes produce currents that depend on the extracellular concentrations of calcium and protons (Uchida et al., 1995; Estevez et al., 2001; Waldegger et al., 2002). We investigated whether the DCT Cl^- channel was also sensitive to these factors using the Na-acetate protocol described above to determine channel activity under two conditions in separate patches. In a first experimental series, we compared NP_o in cell-attached patches formed with pipettes containing nominally zero calcium (no EGTA added) or 5 mM calcium. The results are shown in Fig. 4. Although the NP_o values varied

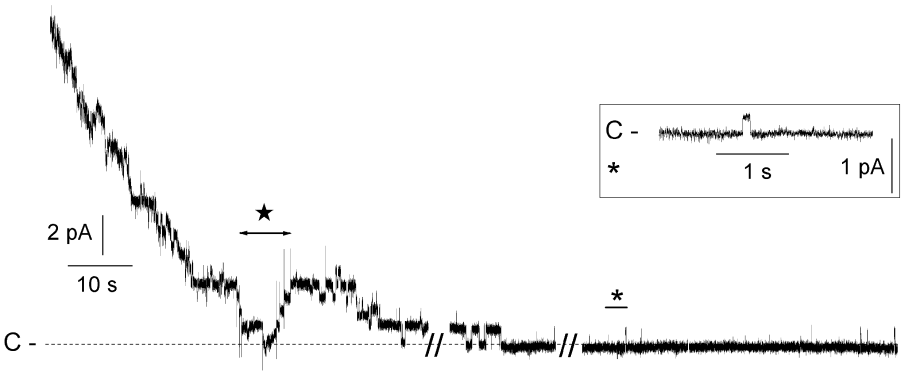

FIGURE 5. Channel rundown occurring after excision. At the beginning of the recording, this inside-out patch had ~15 active channels, but the activity decreased rapidly within 100 s. Subsequently, only brief, isolated openings were recorded, which were maintained for several minutes. This behavior is representative of ~2/3 of the excised patches displaying Cl^- channel activity. The potential was set to 50 mV; the pipette and bath contained PS and low NaCl solution, respectively. The area designated by a star indicates a period in which the voltage varied to establish an i/V_c relationship. The inset is an expanded view of the recording for the area designated by an asterisk. Breaks in the trace: 30 s.

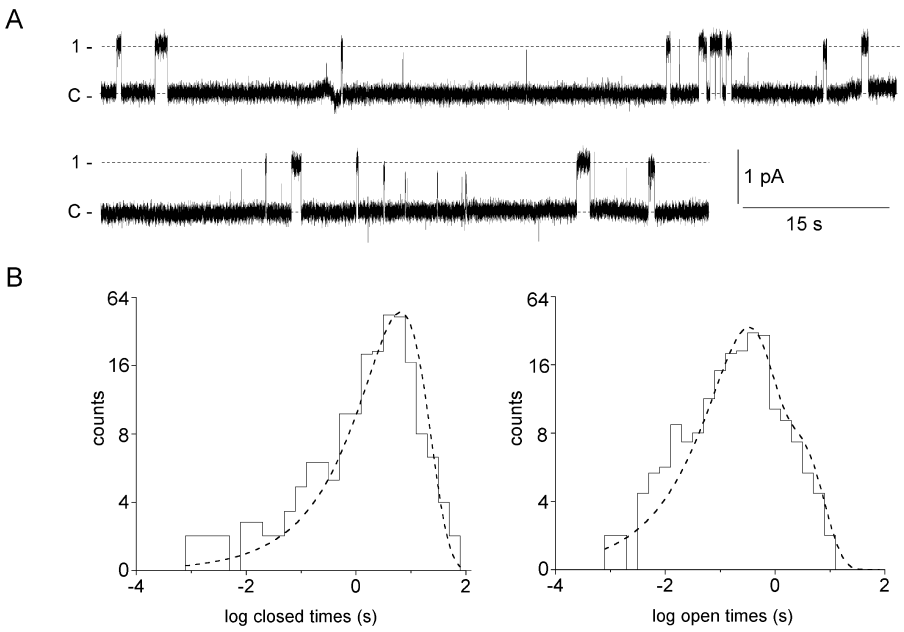

FIGURE 6. Kinetics of the DCT Cl^- channel. (A) Representative recording from one inside-out patch bathed with low NaCl solution lasting ~140 s. The longest opening in this recording lasted 1.65 s and the shortest 0.04 s, with a mean duration of 0.59 s. (B) Stretches of data obtained from 16 inside-out patches bathed with low NaCl solution (PS in the pipette) at 50 mV potential were merged to construct histograms of the channel-open and channel-closed states. The total duration of the recordings was 56 min, and included 374 openings. The number of events per bin (after a square root transformation) is plotted against time (seconds) displayed as a logarithmic function. The lines are fits with one exponential for closed times (time constant: 6.5 s), and with double exponentials for the open times. The two open time constants were 2.2 s (44%) and 0.3 s (56%).

from patch to patch, they were significantly higher in the presence of 5 mM calcium (33.2 ± 5.6, n = 10) than with 0 calcium (11.0 ± 2.9, n = 10, P < 0.002).The decrease in *NPo* (not shown in Fig. 4) resulted exclusively from a significant decrease in the number of channels (N, 40.2 ± 5.5 vs. 14.3 ± 3.5; P < 0.001). The P_o values were not significantly different under these two conditions (0.78 ± 0.05 vs. 0.70 ± 0.05). In contrast, the proportions of patches containing Cl^- channels were similar: there were 72% active patches (total number of patches = 17) under the calcium-free condition versus 62% active patches in the presence of 5 mM calcium (total number of patches = 21). The effects of pH on NP_o (Fig. 4) were more pronounced with NP_o = 2.8 ± 1.0 (n = 9) at pH 6.4 and NP_o = 44.7 ± 8.8 (n = 10, P < 0.001) at pH 8.0. However, in this case, the decrease in NP_o resulted from significant reductions (P < 0.001) in both N (5.3 ± 1.9 vs. 49.3 ± 9.5) and P_o (0.48 ± 0.08 vs. 0.88 ± 0.02). The proportions of patches containing Cl^- channels were once again similar in the two situations: 58% (total number of patches = 19) at pH 6.4 and 54% (total number of patches = 26) at pH 8.0. Neither the extracellular pH nor the external calcium level had any effect on the unit current amplitude at 80 mV (0.66 ± 0.06 pA at pH 6.4 vs. 0.59 ± 0.03 pA at pH 8.0, NS and 0.60 ± 0.01 pA at 5 mM calcium vs. 0.65 ± 0.04 pA at 0 calcium, NS).

Channel Rundown

When we excised patches with Cl^- channel activity in normal PS (containing millimolar concentrations of Mg^{2+} and Ca^{2+}), the channel activity disappeared instantly in most patches. In fact, channel openings were observed in only 6 of 25 excised patches (24%). We an-

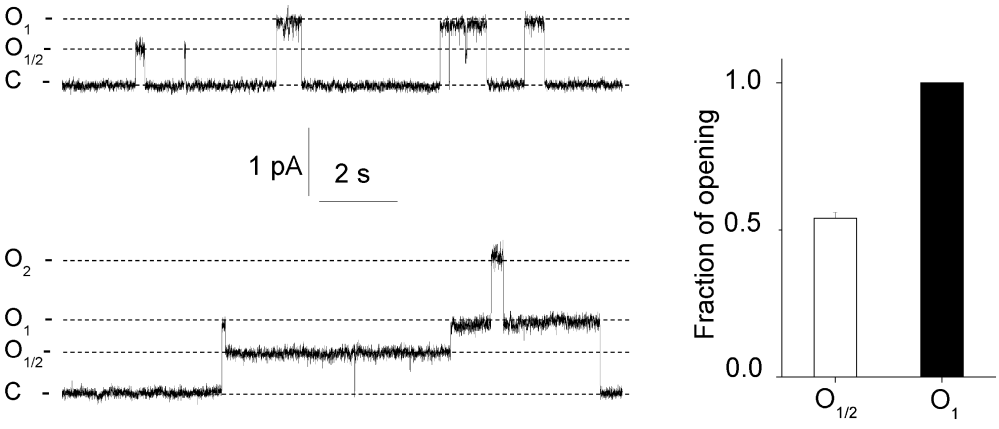

FIGURE 7. Subconductance level of the DCT Cl^- channel. Excerpts of channel current traces recorded from two separate inside-out patches at 50 mV bathed with low NaCl solution (pipette: PS) are shown. C, $O_{1/2}$, O_1, and O_2 denote the closed level, the subconductance level, and complete openings at level one and two, respectively. Histogram of current amplitude of the substate is given as a fraction of the fully open level. The data is averaged from 10 observations.

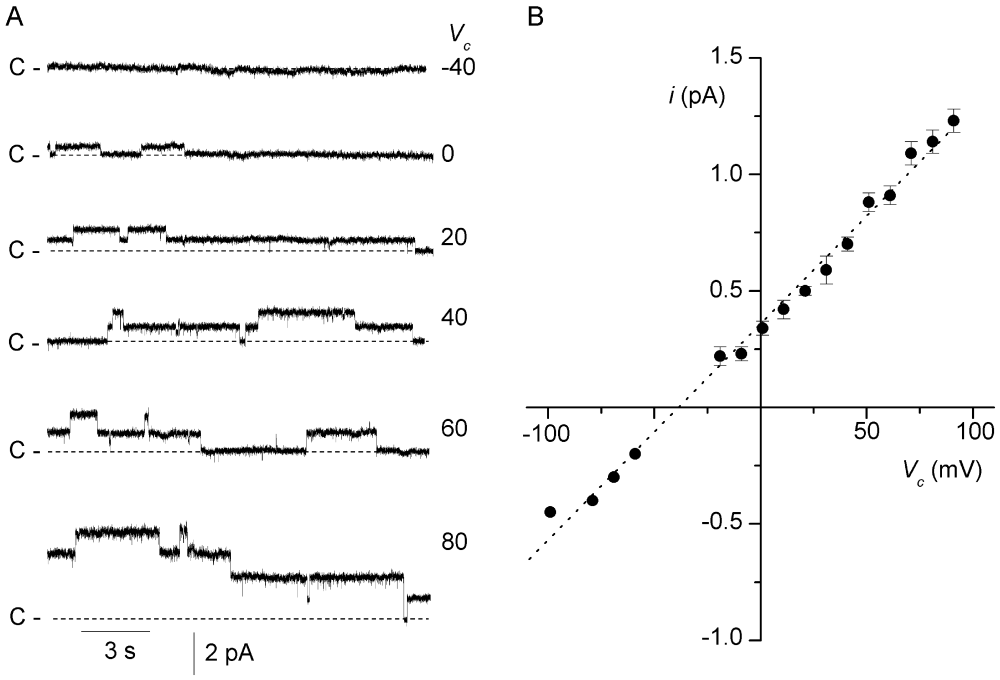

FIGURE 8. Anion versus cation selectivity in the inside-out configuration. (A) Channel current traces recorded from an inside-out patch bathed with low NaCl solution (pipette: PS) at various voltages (V_c, as indicated on the right-hand side of the traces). (B) Current (i)/voltage (V_c) relationships obtained with low NaCl solution (14 mM NaCl) in the bath (pipette: PS). Points are the means of 4–10 measurements from 10 patches, except at $V_c < 0$ mV (two measurements). The line is the linear regression of the data points.

ticipated that the very low frequency of finding an active patch (which contrasts with the abundant presence of the channel in cell-attached patches) might be due to the presence of divalent cations in the bath solution. Indeed, we found that channel activity could be recorded from 31 of 46 patches (67%) when the tubules were superfused with a Ca^{2+}-free solution (no Ca^{2+}, 2 mM EGTA added) before excision. The yield of active patches was no better when the patch membranes were excised in an Mg^{2+} and Ca^{2+}-free solution (no Mg^{2+}, no Ca^{2+}, 2 mM EDTA added, 4 out of 9 patches) or Ca^{2+}-free solution supplemented with 1 mM ATP (5 out of 10 patches). Overall Cl^- channel activity was observed in half of the excised patches (47/90). After isolation, many of the patches showing Cl^- channel activity underwent progressive channel rundown, but the process was quite variable and often incomplete, making it possible to record Cl^- channel activity from excised patches for fairly long periods (exceeding 10–20 min in the most favorable cases). An example of rapid

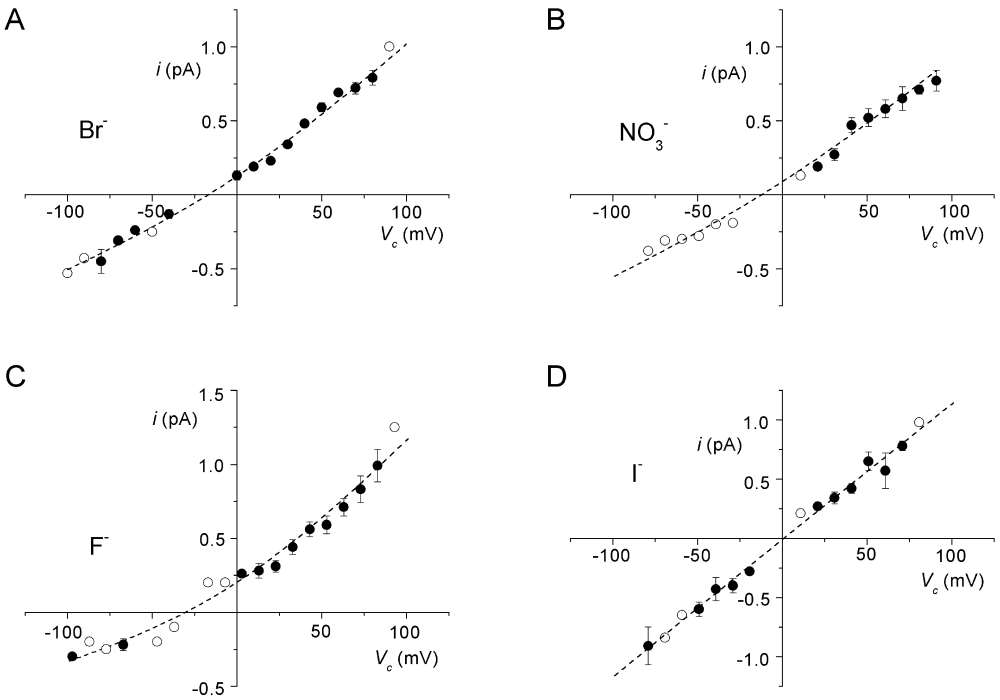

FIGURE 9. Anion selectivity of the DCT Cl^- channel. Current (i)/voltage (V_c) relationships were obtained from inside-out patches under conditions where 130 mM NaCl was replaced by a sodium salt of Br^- (eight patches), NO_3^- (five patches), F^- (five patches) or I^- (four patches). The pipette contained PS. Points are means ± SEM of 3–8 patches (solid circles) or represent two measurements (open circles). The lines are fits with the Goldman-Hodgkin-Katz equation.

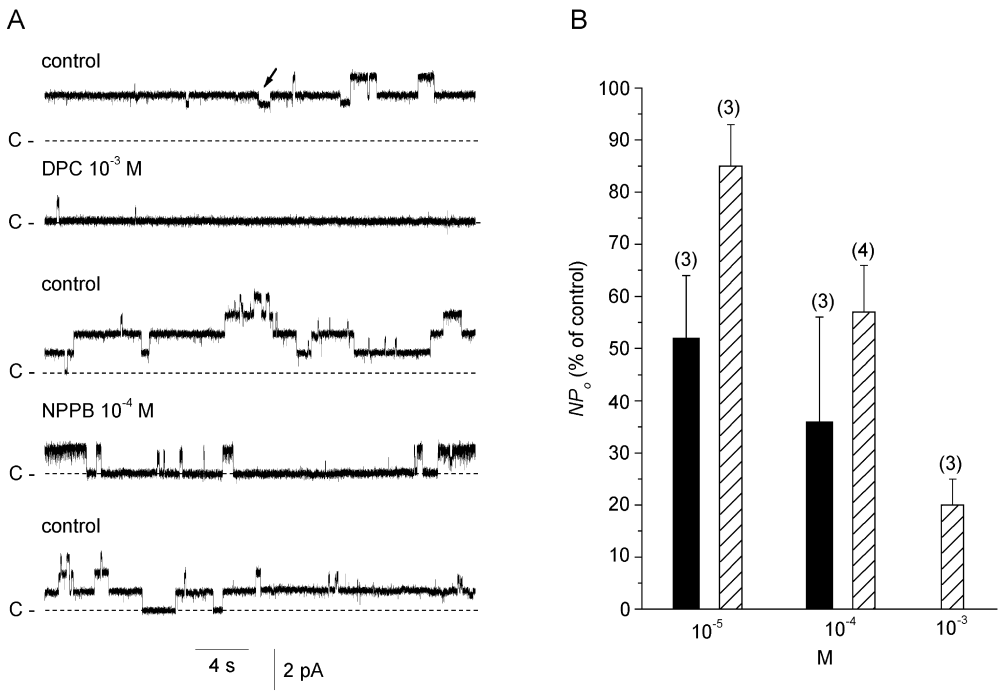

FIGURE 10. Effects of Cl^- channel blockers. (A) Channel current traces extracted from one continuous recording from an inside-out patch showing the effects of NPPB (10^{-4} M) and DPC (10^{-3} M). In the top control trace, the arrow indicates a subconductance level. (B) Histogram giving the NP_o (in percentage of control) in the presence of NPPB (black bars) or DPC (hatched bars). Numbers between brackets indicate the number of observations. The bath contained low NaCl solution and the pipette solution PS.

channel rundown is shown in Fig. 5. This inside-out patch had ~15 channels at the beginning of the recording; a rapid decrease of channel activity was apparent for the first 30 s, which then slowed down, but channel activity had essentially disappeared within 2 min. However, some residual activity (as illustrated in the inset 2 of Fig. 5) persisted for several more minutes.

Channel Kinetics

Visual inspection of the current traces suggests that the channel follows a very slow kinetic pattern. This feature, the frequent decay of channel activity in inside-out patches and the presence of several channels in most patches, made it difficult to estimate the characteristic parameters for channel opening and closure. We selected 16 recordings from excised patches that showed only one level of opening and we merged all the data. The data recorded over 56 min included 374 openings. One such recording is illustrated in Fig. 6 A. The openings could be fitted with double exponentials (Fig. 6 B) having time constants of 2.2 s (44%) and 0.3 s (56%). The closures were best fitted with one exponential (time constant: 6.5 s).

Current Sublevels

We quite often observed a subconductance level of the DCT Cl^- channel. In the cell-attached configuration, complete i-V_c relationships for full and partial openings were obtained in three cases; the unit conductances were 10.7 ± 0.3 pS and 5.5 ± 0.15 pS, for full and partial openings, respectively. The conductance ratio was 0.51 ± 0.01 (n = 3). Similar subconductance levels were also observed in excised patches, usually appearing as partial closures of a full opening, but also, less frequently, as an isolated, partial opening (see Fig. 7). The subconductance level observed in excised patches was 0.54 ± 0.01, i.e., as great as the full opening (n = 10 patches). Under two circumstances, the occurrence of the subconductance levels was sufficiently frequent to establish i-V_c relationships for the 1/2 and full amplitudes in the same patch in low NaCl solution. This made it possible to check that the two levels had similar P_{Na}/P_{Cl} ratios (unpublished data).

Conductance and Ion Selectivity

With PS on both sides of the membrane patch, the i-V_m relationship measured in the excised mode was linear, and the unit conductance (g = 10.7 ± 1.1 pS, n = 6) was not statistically different from that determined in the cell-attached configuration (9.5 ± 0.3 pS, n = 25, P = 0.14). With the low NaCl solution as bath solution, and PS in the pipette, the i-V_c relationship was shifted to the left, indicating anionic selectivity (Fig. 8). The individual P_{Na}/P_{Cl} values were calculated from E_r because, in all but three cases, we did not succeed in detecting channel openings at $V_c < E_r$. The mean E_r was −40.3 ± 1.6 mV (n = 10) and P_{Na}/P_{Cl}, 0.09 ± 0.04 (n = 10). In the three cases for which current values could be measured at $V_c < Er$, the data points were fitted to the current Goldman-Hodgkin-Katz equation (see MATERIALS AND METHODS) and yielded a somewhat higher value of 0.13 ± 0.09 (n = 3).

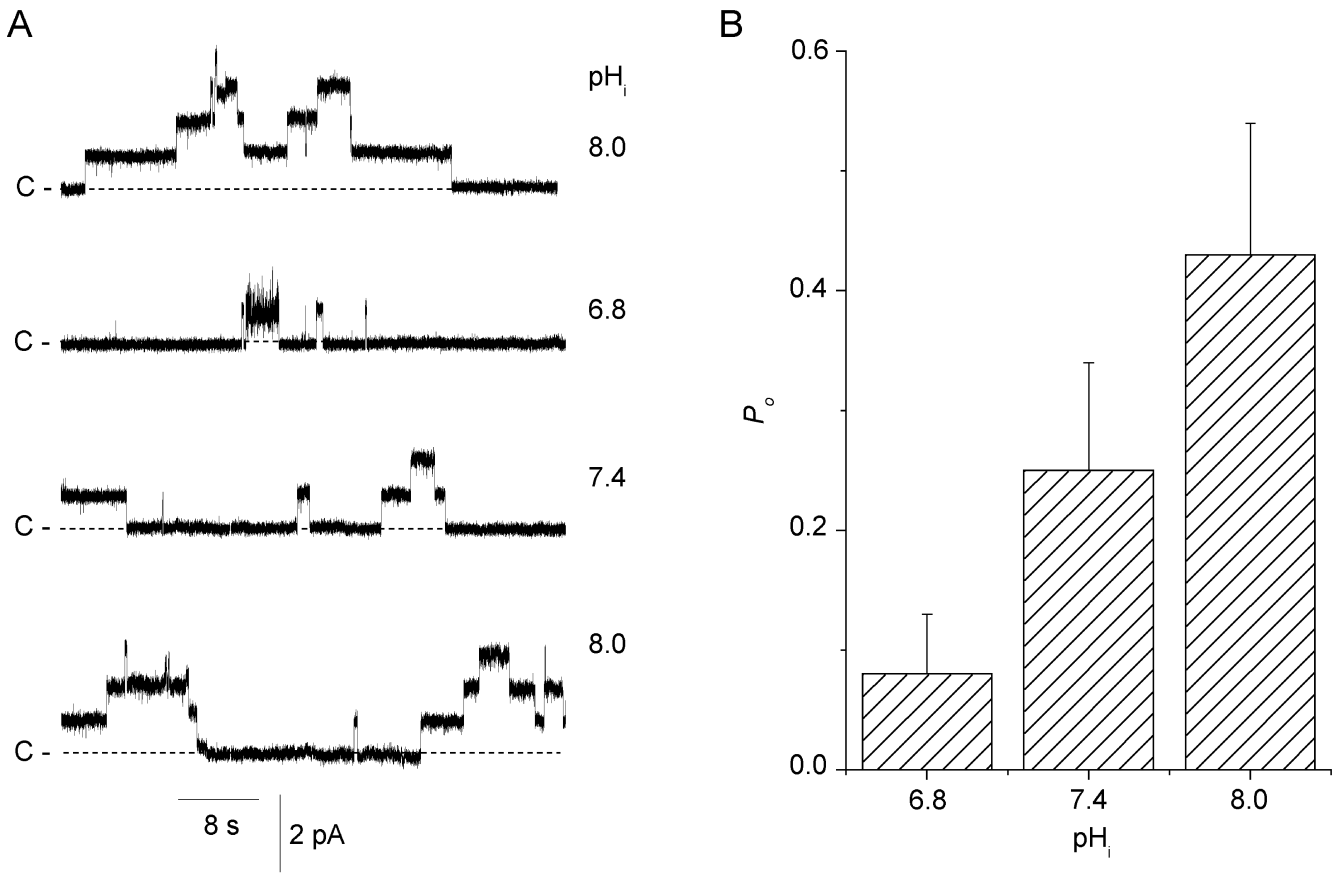

FIGURE 11. Effects of intracellular pH on Cl^- channel activity. (A) Channel current traces showing that channel activity decreased at acid pH, and increased at alkaline pH. The recording was done at 50 mV in the inside-out configuration, with low NaCl solution on the inner side of the membrane patch and PS in the pipette. The value of the intracellular pH (pH_i) is indicated on the right hand side of the tracings. No decrease in channel amplitude is apparent. (B) Histogram for the effects of pH_i on the open probability (*Po*). Each bar is the mean of six measurements.

The selectivity among anions was assessed from *i-V$_c$* measurements when most of the chloride in the bathing solution (i.e., 130 mM) was replaced by the test anion. The mean *i-V$_c$* relationships are shown in Fig. 9 for bromide (A), nitrate (B), fluoride (C), and iodide (D). We were only able to detect current openings at $V_c < E_r$ for 2/5 patches during NO_3^- substitution and for 4/8 during Br^- substitution. For this reason, the relative permeabilities were assessed by measuring E_r after linear regression. We obtained comparable values for both ions: $P_{Br}/P_{Cl} = 0.43 \pm 0.08$ ($n = 8$) and $P_{NO3}/P_{Cl} = 0.53 \pm 0.06$ ($n = 5$). In the cases for which current values could be measured at $V_c < Er$, the data points were fitted with the current Goldman-Hodgkin-Katz equation (see MATERIALS AND METHODS) and yielded comparable figures (P_{Br}/P_{Cl}: 0.41 ± 0.05, $n = 4$; P_{NO3}/P_{Cl}: 0.53 and 0.56). Current openings were readily measured at $V_c < E_r$ when testing iodide and fluoride; therefore, the data were fitted with the Goldman-Hodgkin-Katz equation, and yielded $P_I/P_{Cl} = 0.87 \pm 0.06$ ($n = 4$) and $P_F/P_{Cl} = 0.15 \pm 0.03$ ($n = 5$). Thus, in summary, the permeability sequence was $Cl^- \sim I^- > Br^- \sim NO_3^- > F^-$.

Blockade of the Channel

The effects of internal NPPB, DPC, and DIDS were tested in inside-out patches. Fig. 10 A illustrates the effects of NPPB and DPC on Cl^- channels recorded from one inside-out patch bathed with low NaCl solution. The results are summarized in Fig. 10 B. NPPB at 10^{-4} M and DPC at 10^{-3} M only partly inhibited the channel, reducing NP_o to 36 ± 20% ($n = 3$) and 20 ± 5% ($n = 4$), respectively. DIDS (10^{-3} M, 3 patches) had no clear inhibitory effect (unpublished data).

Effects of Internal pH, Calcium, ATP and PKA

We examined the effects of the intracellular pH on inside-out membrane patches, at 6.8, 7.4, and 8.0. Whenever it was possible, measurements at 6.8 and 8.0 were bracketed by measurements at pH 7.4. A representative experiment is shown in Fig. 11 A. In that case, the P_o at pH 8.0 was 3.5 times higher than the control P_o at pH

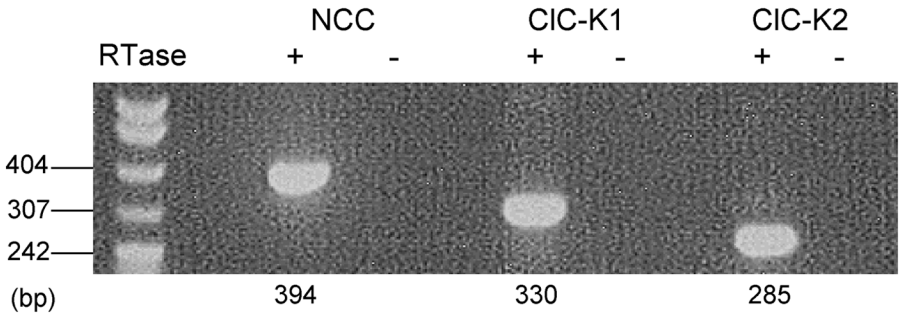

FIGURE 12. Sample gel showing that ClC-K1 and ClC-K2 mRNAs are expressed in mouse DCT. The mRNA of the Na^+-Cl^- cotransporter (NCC) was used as the control in each experiment. + and −, samples were treated with reverse transcriptase (RTase) or untreated, respectively. For all sequences, the RT-PCR reaction was performed on an aliquot of the same RNA extracts (2.5 μl, corresponding to 0.2 mm tubule length per PCR tube). Similar results were obtained with different extracts in three other experiments.

7.4 and the P_o at pH 6.8 was 3.5 times lower than the control P_o at pH 7.4. The mean results (n = 6) are shown in a histogram (Fig. 11 B). The unit current amplitudes were not altered (unpublished data). We have already mentioned that excising the membrane patches in the presence of millimolar Ca^{2+} bath resulted in the immediate loss of channel activity for most patches (see channel rundown section). However, once the patches had been isolated in a Ca^{2+}-free solution, intracellular Ca^{2+} (at concentrations up to 10^{-6} M) no longer had any effect on Cl^- channel activity, since the NP_o measured in the presence of 10^{-7} M or 10^{-6} M calcium (n = 3) were 97 ± 3% and 97 ± 5% of control (in the presence of 10^{-9} M calcium).

The DCT Cl^- channel was not activated in the presence of intracellular ATP (n = 12) and was not further stimulated by applying the catalytic subunit of the protein kinase A at the inner side of the patch (n = 5).

RT-PCR Detection of mRNAs for ClC-K1 and ClC-K2

RT-PCR was performed on microdissected DCTs to confirm the presence of ClC-K channels (Fig. 12). Like Kieferle et al. (1994), but unlike other authors (Adachi et al., 1994; Uchida et al., 1995; Yoshikawa et al., 1999; Kobayashi et al., 2001), we found that the mRNAs for both ClC-K1 and ClC-K2 were present in the mouse DCT.

DISCUSSION

Properties of the DCT Cl^- Channel

This novel Cl^- channel, recorded on the basolateral membrane of the DCT, has properties that distinguish it from several Cl^- channel types. First, the unit conductance is intermediate, much lower than the conductances of the maxi Cl^- channel and the outwardly rectifying Cl^- channel, but higher than the conductances of the calcium-dependent Cl^- channel and several ClC channels (Jentsch et al., 2002), and more alike CFTR unit conductance. Second, with an anionic selectivity sequence $Cl^- \sim I^- > Br^- \sim NO_3^- > F^-$, the DCT Cl^- channel differs from most endogenously identified Cl^- channels (Qu and Hartzell, 2000), including the CFTR (Dawson et al., 1999). The anionic permeability sequence resembles that of ClC channels when it has been measured ($Cl^- > Br^-$) (Fahlke, 2001).

In addition, the DCT Cl^- channel, unlike two major classes of Cl^- channels, is insensitive to intracellular calcium and cyclic AMP. Besides the modulating effect of intracellular pH, frequently observed in many channels, the stimulatory effects of extracellular pH and calcium could represent a distinctive signature of this type of channel. Indeed, similar properties have been reported for the Cl^- conductance in the thin ascending limb using the isolated, microperfused tubule technique (Kondo et al., 1987, 1988), and later been retrieved from ClC-K channels (Uchida et al., 1993, 1995; Estevez et al., 2001; Waldegger et al., 2002). In our study, the effects of external pH were more pronounced than those of external calcium (as observed for ClC-K2), and this seems to imply primarily a reduction in the number of active channels, even though a moderate decrease of P_o was observed at acid pH. Quite similar effects of external pH and calcium have been reported recently on Cl^- channels reconstituted in artificial membrane bilayers using membrane vesicles from the rabbit distal nephron (Sauvé et al., 2000). In contrast to our results, however, the inhibition produced by acid pH and low calcium were due to a major decrease in P_o, and a huge increase in calcium (>20 mM) was necessary to reveal any modulation of channel activity by external calcium. The physiological relevance of pH and calcium modulation remains to be investigated, but this type of regulation seems to offer a useful tool for classifying Cl^- channels in the kidney. Despite quantitative differences, which probably reflect the different methodologies used in our study and that by Sauvé et al. (2000), these two studies both strongly suggest that Cl^- channels of the ClC-K type are present in the distal tubule.

The pharmacology of the DCT Cl^- channel cannot easily be compared with that of ClC-Ks. The few studies

that have looked for ClC-K blockers used the oocyte expression system and voltage clamp. This means that all agents were applied to the extracellular side, whereas in our study they were applied intracellularly. NPPB has not been tested on ClC-Ks. The membrane permeant DPC (1 mM) produced only a slight blockade of rat ClC-K2 (Adachi et al., 1994), but almost completely blocked the Cl^- conductance induced in oocytes by injecting mRNA isolated from the outer medulla of rabbit kidney (Zimniak et al., 1992). This conductance is probably attributable to ClC-Ks (Reeves et al., 2001). Extracellular DIDS (0.5–1 mM) blocked both ClC-K1 (Uchida et al., 1993; Waldegger and Jentsch, 2000) and ClC-K2 (Adachi et al., 1994); however, DIDS is not membrane permeant. There have been reports of that DIDS blocks Cl^- conductance from one side of the membrane but not from the other (Chesnoy-Marchais, 1983).

The occurrence of 1/2 sublevel openings is obviously reminiscent of the fact that ClC channels have two pores with similar conductances (Maduke et al., 2000). However, under the conditions used throughout these experiments, transitions from half-opening to complete closure were very rare and brief, suggesting that the P_o of the two hypothetical independent pores were close to one. This contrasts with the behavior of ClC-0, as reported by Miller and White (1984) and Ludewig et al. (1997), where the channel clearly fluctuates between a nonconducting level and two equally spaced conducting levels (at least at the most negative voltages). We were unable to increase the number of transitions from 1/2 sublevels to complete closing level by changing the recording conditions (decrease of Cl^- concentration, changes in pH, perfusion of intracellular DIDS). Thus, half-amplitude openings may as well represent a classical substate of the channel. However, the strikingly slow kinetics of the channel, with openings in the second range, is to some extent reminiscent of the common gate demonstrated for ClC-0, which also has slow kinetics (Maduke et al., 2000). This characteristic supports the notion that the DCT Cl^- channel is a double-pore channel, the activity of which is primarily determined by the common gate. This, of course, requires further investigation.

Comparison with Other Renal Chloride Channels

Only a few Cl^- channels have been identified in the native renal tubule by the means of the patch-clamp technique. Our laboratory has characterized two channels in the thick ascending limb (see Table I). A 45-pS channel (Paulais and Teulon, 1990) is probably similar to the one reported by Reeves and Andreoli in their studies using artificial membrane bilayers (Reeves et al., 2001). The second channel (Guinamard et al., 1995) has lower conductance (9 pS) and an anionic selectivity sequence of $Br^- > NO_3^- > Cl^- > F^-$. It is sensitive to intracellular pH (Guinamard et al., 1996) and is stimulated by ATP, PKA (Guinamard et al., 1995), and pyrophosphate (Marvao et al., 1998). A quite similar channel has been found on the basolateral membrane of the rabbit proximal tubule (Segal et al., 1993). The DCT Cl^- channel is obviously distinct from the 45-pS channel, but it also has properties that are quite distinct from those of the smaller Cl^- channel in terms of anionic selectivity and sensitivities to ATP and PKA. In addition, although both channels are inhibited by DPC and NPPB, the DCT Cl^- channel seems to be less sensitive to these agents. Some other Cl^- channels have been recorded on the apical membranes of cultured renal cells (see Schwiebert et al., 1994), including PKA-activated CFTR-like Cl^- channels (Poncet et al., 1994), all of which differ from the channel under study. Overall, therefore, the DCT Cl^- channel stands out from all the Cl^- channels described to date in the native renal tubule and cultured cells, and only shares some properties with the Cl^- channel reconstituted into artificial membrane bilayers mentioned in the previous section (Sauvé et al., 2000). However, it is noteworthy that this latter channel, unlike the DCT Cl^- channel, is stimulated by PKA and seems to be embedded within the apical membrane (Denicourt et al., 1996). The anionic selectivity is not known.

TABLE I

Chloride Channels of the Mouse Renal Tube

Tubule	g	P_{Na}/P_{Cl}	P_{Br}	P_{NO3}	P_F	P_I	Alkaline pH_i	ATP_i	PKA
	pS								
CTAL	45	0.05	0.7	0.4	0.03	?	−	−	−
CTAL	9	0.10	1.1	1.3	0.4	1.6	+	+	+
DCT	9.5	0.09	0.4	0.5	0.1	0.9	+	−	−

This table summarizes the results on basolateral Cl^- channels derived from experiments on microdissected mouse renal tubules. Data for CTAL are from Paulais and Teulon (1990) and Guinamard et al. (1995, 1996). Activation and lack of effect of the designated agents are indicated by + and −, respectively. DCT, distal convoluted tubule; CTAL, cortical thick ascending limb; pH_i and ATP_i, intracellular pH and ATP; PKA, catalytic subunit of protein kinase A.

Molecular Identity of the DCT Chloride Channel

The molecular identity of the DCT Cl^- channel has obviously not been determined by our study, but several reports in the literature reasonably identify the ClC-Ks as the most likely candidates. After RT-PCR measurements on microdissected tubular fragments from the rat and mouse kidneys (Adachi et al., 1994; Kieferle et al., 1994; Yoshikawa et al., 1999; Kobayashi et al., 2001), there is general agreement that ClC-K2 is present in the DCT, whereas the presence of ClC-K1 is denied by

Uchida et al. (1995). Our RT-PCR data, like those reported by others (Kieferle et al., 1994; Vandewalle et al., 1997; Waldegger et al., 2002), indicate that CLC-K1 is present in the DCT. It has also been shown that the ClC-Ks are located on the basolateral membrane of the renal tubule (Vandewalle et al., 1997; Kobayashi et al., 2001), as required for channels implicated in the absorption of Cl^-, and as observed for our channel. In addition, as alluded to before, recent electrophysiological evidence indicates that the activities of ClC-K1 and ClC-K2 are increased in the presence of high extracellular pH or calcium, and the permeability sequence of the DCT Cl^- channel is similar to that of ClC-K2, with the exception of iodide.

Thus, our study on microdissected DCTs demonstrates the presence of an abundant Cl^- channel in the basolateral membrane, which has features compatible with a ClC-K2 channel and constitues a new functional type of Cl^- channel. From a physiological point of view, the regulatory properties of the channel have two main implications. On the one hand, our results suggest that NaCl absorption in the DCT could be negatively regulated by PKC acting on the Cl^- channel. This property will require further investigation. On the other hand, with regard to the positive regulation of NaCl absorption, our data rule out the possibility that cyclic AMP regulates this channel, although it has been suggested that cyclic AMP may stimulate NaCl absorption across the DCT (see Reilly and Ellison, 2000). Some other factor must therefore help to adapt channel activity to the luminal entry of Cl^- mediated by the Na^+-Cl^- cotransport, particularly because NaCl transport is primarily determined by the load of NaCl delivered to the DCT lumen (Reilly and Ellison, 2000). In the light of our findings, one possible candidate is the pH_i. However, the simplest hypothesis would be that the intracellular Cl^- itself controls the channel. Modulation of this type has previously been reported for another renal Cl^- channel (Reeves et al., 2001).

We wish to thank Martine Imbert-Teboul (CNRS FRE 2468, Paris) for help in obtaining RT-PCR measurements. The English text has been checked by Monika Ghosh.

S. Lourdel holds a PhD fellowship from the Ministère de la Recherche and M. Paulais is an INSERM researcher.

Olaf S. Andersen served as editor.

Submitted: 25 October 2002
Revised: 7 February 2003
Accepted: 27 February 2003

REFERENCES

Adachi, S., S. Uchida, H. Ito, M. Hata, M. Hiroe, F. Marumo, and S. Sasaki. 1994. Two isoforms of a chloride channel predominantly expressed in thick ascending limb of Henle's loop and collecting ducts of rat kidney. *J. Biol. Chem.* 269:17677–17683.

Barry, P.H., and J.W. Lynch. 1991. Liquid junction potentials and small cell effects in patch-clamp analysis. *J. Membr. Biol.* 121:101–117.

Chesnoy-Marchais, D. 1983. Characterization of a chloride conductance activated by hyperpolarization in Aplysia neurones. *J. Physiol.* 342:277–308.

Chomczynski, P., and N. Sacchi. 1987. Single step method of RNA isolation by acid guanidium thiocyanate-phenol-chloroform extraction. *Anal. Biochem.* 162:156–159.

Chraibi, A., T. Van den Abbeele, R. Guinamard, and J. Teulon. 1994. A ubiquitous non-selective cation channel in the mouse renal tubule with variable sensitivity to calcium. *Pflugers Arch.* 429: 90–97.

Dawson, D.C., S.S. Smith, and M.K. Mansoura. 1999. CFTR: mechanism of anion conduction. *Physiol. Rev.* 79:S47–S75.

Denicourt, N., S. Cai, L. Garneau, M.G. Brunette, and R. Sauvé. 1996. Evidence from incorporation experiments for an anionic channel of small conductance at the apical membrane of the rabbit distal tubule. *Biochim. Biophys. Acta.* 1285:155–166.

Estevez, R., T. Boettger, V. Stein, R. Birkenhager, E. Otto, F. Hildebrandt, and T.J. Jentsch. 2001. Barttin is a Cl^- channel beta-subunit crucial for renal Cl^- reabsorption and inner ear K^+ secretion. *Nature.* 414:558–561.

Fahlke, C. 2001. Ion permeation and selectivity in ClC-type chloride channels. *Am. J. Physiol. Renal Physiol.* 280:F748–F757.

Greger, R., and H. Velazquez. 1987. The cortical thick ascending limb and early distal convoluted tubule in the urinary concentrating mechanism. *Kidney Int.* 31:590–596.

Guinamard, R., A. Chraibi, and J. Teulon. 1995. A small-conductance Cl^- channel in the mouse thick ascending limb that is activated by ATP and protein kinase A. *J. Physiol.* 485:97–112.

Guinamard, R., M. Paulais, and J. Teulon. 1996. Inhibition of a small-conductance cAMP-dependent Cl^- channel in the mouse thick ascending limb at low internal pH. *J. Physiol.* 490:759–765.

Hamill, O.P., A. Marty, E. Neher, B. Sakmann, and F.J. Sigworth. 1981. Improved patch-clamp techniques for high-resolution current recording from cells and cell-free membrane patches. *Pflugers Arch.* 391:85–100.

Jentsch, T.J., V. Stein, F. Weinreich, and A.A. Zdebik. 2002. Molecular structure and physiological function of chloride channels. *Physiol. Rev.* 82:503–568.

Kieferle, S., P. Fong, M. Bens, A. Vandewalle, and T.J. Jentsch. 1994. Two highly homologous members of the ClC chloride channel family in both rat and human kidney. *Proc. Natl. Acad. Sci. USA.* 91:6943–6947.

Kobayashi, K., S. Uchida, S. Mizutani, S. Sasaki, and F. Marumo. 2001. Intrarenal and cellular localization of CLC-K2 protein in the mouse kidney. *J. Am. Soc. Nephrol.* 12:1327–1334.

Kondo, Y., K. Yoshitomi, and M. Imai. 1987. Effect of pH on Cl^- transport in TAL of Henle's loop. *Am. J. Physiol.* 253:F1216–F1222.

Kondo, Y., K. Yoshitomi, and M. Imai. 1988. Effect of Ca^{2+} on Cl^- transport in thin ascending limb of Henle's loop. *Am. J. Physiol.* 254:F232–F239.

Konrad, M., M. Vollmer, H.H. Lemmink, L.P. van den Heuvel, N. Jeck, R. Vargas-Poussou, A. Lakings, R. Ruf, G. Deschenes, C. Antignac, et al. 2000. Mutations in the chloride channel gene CLCNKB as a cause of classic Bartter syndrome. *J. Am. Soc. Nephrol.* 11:1449–1459.

Loffing, J., D. Loffing-Cueni, V. Valderrabano, L. Klausli, S.C. Hebert, B.C. Rossier, J.G. Hoenderop, R.J. Bindels, and B. Kaissling. 2001. Distribution of transcellular calcium and sodium transport pathways along mouse distal nephron. *Am. J. Physiol.* 281:F1021–F1027.

Lourdel, S., M. Paulais, F. Cluzeaud, M. Bens, M. Tanemoto, Y. Kurachi, A. Vandewalle, and J. Teulon. 2002. An inward rectifier K^+ channel at the basolateral membrane of the mouse distal convoluted tubule: similarities with Kir4-Kir5.1 heteromeric channels.

J. Physiol. 538:391–404.

Ludewig, U., M. Pusch, and T.J. Jentsch. 1997. Independent gating of single pores in CLC-0 chloride channels. *Biophys. J.* 73:789–797.

Maduke, M., C. Miller, and J.A. Mindell. 2000. A decade of CLC chloride channels: structure, mechanism, and many unsettled questions. *Annu. Rev. Biophys. Biomol. Struct.* 29:411–438.

Marvao, P., M.-C. De Jesus Ferreira, C. Bailly, M. Paulais, R. Guinamard, M. Bens, R. Moreau, A. Vandewalle, and J. Teulon. 1998. Cl^- absorption across the thick ascending limb is not altered in cystic fibrosis mice. A role for a pseudo CFTR Cl^- channel. *J. Clin. Invest.* 102:1986–1993.

Miller, C., and M.M. White. 1984. Dimeric structure of single chloride channels from Torpedo electroplax. *Proc. Natl. Acad. Sci. USA.* 81:2772–2775.

Paulais, M., and J. Teulon. 1990. cAMP-activated chloride channel in the basolateral membrane of the thick ascending limb of the mouse kidney. *J. Membr. Biol.* 113:253–260.

Poncet, V., M. Tauc, M. Bidet, and P. Poujeol. 1994. Chloride channels in apical membrane of primary cultures of rabbit distal bright convoluted tubule. *Am. J. Physiol.* 266:F543–F553.

Qu, Z., and H.C. Hartzell. 2000. Anion permeation in Ca^{2+}-activated Cl^- channels. *J. Gen. Physiol.* 116:825–844.

Reeves, W.B., C.J. Winters, and T.E. Andreoli. 2001. Chloride channels in the loop of Henle. *Annu. Rev. Physiol.* 63:631–645.

Reilly, R.F., and D.H. Ellison. 2000. Mammalian distal tubule: physiology, pathophysiology, and molecular anatomy. *Physiol. Rev.* 80: 277–313.

Robinson, R.A., and R.H. Stokes. 1965. Electrolyte solutions. 2nd edition. Butterworths, London, UK.

Rubera, I., M. Tauc, C. Poujeol, M.T. Bohn, M. Bidet, G. De Renzis, and P. Poujeol. 1997. Cl^- and K^+ conductances activated by cell swelling in primary cultures of rabbit distal bright convoluted tubules. *Am. J. Physiol.* 273:F680–F697.

Rubera, I., M. Tauc, C. Verheecke-Mauze, M. Bidet, C. Poujeol, N. Touret, B. Cuiller, and P. Poujeol. 1999. Regulation of cAMP-dependent chloride channels in DC1 immortalized rabbit distal tubule cells in culture. *Am. J. Physiol.* 276:F104–F121.

Sauvé, R., S. Cai, L. Garneau, H. Klein, and L. Parent. 2000. pH and external Ca^{2+} regulation of a small conductance Cl^- channel in kidney distal tubule. *Biochim. Biophys. Acta.* 1509:73–85.

Schwiebert, E., A. Lopes, and W. Guggino. 1994. Chloride channels along the nephron. *In* Chloride Channels. W. Guggino, editor. Academic Press, New York. 265–316.

Segal, A.S., J. Geibel, and E.L. Boulpaep. 1993. A chloride channel resembling CFTR on the basolateral membrane of rabbit proximal tubule. *J. Am. Soc. Nephrol.* 4:879a.

Simon, D.B., R.S. Bindra, T.A. Mansfield, C. Nelson-Williams, E. Mendonca, R. Stone, S. Schurman, A. Nayir, H. Alpay, A. Bakkaloglu, et al. 1997. Mutations in the chloride channel gene, CLCNKB, cause Bartter's syndrome type III. *Nat. Genet.* 17:171–178.

Uchida, S. 2000. In vivo role of CLC chloride channels in the kidney. *Am. J. Physiol. Renal Physiol.* 279:F802–F808.

Uchida, S., S. Sasaki, T. Furukawa, M. Hiraoka, T. Imai, Y. Hirata, and F. Marumo. 1993. Molecular cloning of a chloride channel that is regulated by dehydration and expressed predominantly in kidney medulla. *J. Biol. Chem.* 268:3821–3824.

Uchida, S., S. Sasaki, K. Nitta, K. Uchida, S. Horita, H. Nihei, and F. Marumo. 1995. Localization and functional characterization of rat kidney-specific chloride channel, ClC-K1. *J. Clin. Invest.* 95: 104–113.

Vandewalle, A., F. Cluzeaud, M. Bens, S. Kieferle, K. Steinmeyer, and T.J. Jentsch. 1997. Localization and induction by dehydration of ClC-K chloride channels in the rat kidney. *Am. J. Physiol.* 272:F678–F688.

Waldegger, S., N. Jeck, P. Barth, M. Peters, H. Vitzthum, K. Wolf, A. Kurtz, M. Konrad, and H.W. Seyberth. 2002. Barttin increases surface expression and changes current properties of ClC-K channels. *Pflugers Arch.* 444:411–418.

Waldegger, S., and T.J. Jentsch. 2000. Functional and structural analysis of ClC-K chloride channels involved in renal disease. *J. Biol. Chem.* 275:24527–24533.

Wang, T., S.K. Agulian, G. Giebisch, and P.S. Aronson. 1993. Effects of formate and oxalate on chloride absorption in rat distal tubule. *Am. J. Physiol.* 264:F730–F736.

Yoshikawa, M., S. Uchida, A. Yamauchi, A. Miyai, Y. Tanaka, S. Sasaki, and F. Marumo. 1999. Localization of rat CLC-K2 chloride channel mRNA in the kidney. *Am. J. Physiol.* 276:F552–F558.

Yoshitomi, K., T. Shimizu, J. Taniguchi, and M. Imai. 1989. Electrophysiological characterization of rabbit distal convoluted tubule cell. *Pflugers Arch.* 414:457–463.

Zimniak, L., W.B. Reeves, and T.E. Andreoli. 1992. Cl^- channels in basolateral renal medullary membranes. VI. Cl^- conductance expression in *Xenopus* oocytes. *Am. J. Physiol.* 263:F979–F984.